Optical measurement of arterial mechanical properties: from atherosclerotic plaque initiation to rupture

Journal of Biomedical Optics

SPIEDigitalLibrary.org/jbo

Optical measurement of arterial mechanical properties: from atherosclerotic plaque initiation to rupture

Seemantini K. Nadkarni

SPIE

Journal of Biomedical Optics 18(12), 121507 (December 2013)

REVIEW

Optical measurement of arterial mechanical properties: from atherosclerotic plaque initiation to rupture

Seemantini K. Nadkarni
Massachusetts General Hospital, Harvard Medical School, Wellman Center for Photomedicine, Boston, Massachusetts 02114

Abstract. During the pathogenesis of coronary atherosclerosis, from lesion initiation to rupture, arterial mechanical properties are altered by a number of cellular, molecular, and hemodynamic processes. There is growing recognition that mechanical factors may actively drive vascular cell signaling and regulate atherosclerosis disease progression. In advanced plaques, the mechanical properties of the atheroma influence stress distributions in the fibrous cap and mediate plaque rupture resulting in acute coronary events. This review paper explores current optical technologies that provide information on the mechanical properties of arterial tissue to advance our understanding of the mechanical factors involved in atherosclerosis development leading to plaque rupture. The optical approaches discussed include optical microrheology and traction force microscopy that probe the mechanical behavior of single cell and extracellular matrix components, and intravascular imaging modalities including laser speckle rheology, optical coherence elastography, and polarization-sensitive optical coherence tomography to measure the mechanical properties of advanced coronary lesions. Given the wealth of information that these techniques can provide, optical imaging modalities are poised to play an increasingly significant role in elucidating the mechanical aspects of coronary atherosclerosis in the future. [DOI: 10.1117/1.JBO.18.12.121507]

Keywords: mechanical properties; plaque rupture; atherosclerosis; speckle rheology; microrheology; elastography.

Paper 130558SSR received Aug. 2, 2013; revised manuscript received Oct. 9, 2013; accepted for publication Oct. 10, 2013; published online Dec. 2, 2013.

1 Introduction

Despite major advances in coronary interventions and pharmacotherapies, acute myocardial infarction (AMI) remains the leading cause of death, annually claiming more lives worldwide than all cancers, accidents, and AIDS combined. Autopsy studies reveal a type of plaque, the thin cap fibroatheroma (TCFA), implicated at the site of culprit thrombi in >70% of patients who have succumbed to AMI.[1,2] Unstable TCFAs are most frequently found within the proximal ~5 cm of the major coronary arteries and are histologically hallmarked by the presence of a thin fibrous cap, rich in macrophages, overlying a large necrotic lipid pool. Motivated by the compelling clinical need to detect unstable plaques, a number of technologies such as optical coherence tomography (OCT), virtual histology intravascular ultrasound (VH-IVUS), computed tomography, angioscopy, and near-infrared spectroscopy (NIRS) have been investigated in patients to evaluate key morphologic features such as fibrous cap thickness, plaque burden, calcific nodules, and lipid content.[3–5] A critical challenge, however, in identifying plaques with the highest risk of rupture is that plaques with similar unstable morphologic features do not all possess an equal likelihood of rupture. For example, in 70% of patients dying from AMI, multiple TCFAs are found without rupture at sites remote from the culprit plaque and in nonculprit arteries,[6] and appear with similar frequency in stable patients with asymptomatic coronary artery disease.[6–9] The recent PROSPECT study showed that fibrous cap thickness in itself was not a sufficient predictor of acute events in patients and that increased plaque burden was also an important consideration.[10] Moreover, in ~20% of cases, plaque rupture is observed in necrotic core lesions with thicker fibrous caps (>100 μm), intraplaque hemorrhage, or calcific nodules.[6,8,11,12] These findings call into question a detection paradigm that relies entirely on morphologic criteria and highlight the need to augment morphologic findings with critical surrogate metrics, such as mechanical metrics, in order to accurately evaluate the risk of plaque rupture.[2,6]

The atheroma is viscoelastic in nature, exhibiting both liquid (viscous) and solid (elastic) behavior. During the pathogenesis of atherosclerosis, from lesion initiation to rupture, the viscoelastic properties of the arterial extracellular matrix (ECM) are altered by an intricate milieu of cellular and molecular processes intrinsic to the coronary wall as well as humeral factors. In early lesions, inflammatory processes influence the accumulation of low-viscosity lipid,[13,14] and in advanced plaques, the apoptosis of foam cells and intraplaque hemorrhage results in large necrotic lipid pools of further reduced viscosity.[15,16] The mechanical properties of the atheroma determine the extent of induced deformations or strains in response to extrinsic hemodynamic stresses. Higher strains are measured in lipid-rich regions of lower viscosity,[17] and cyclic mechanical strain within the arterial wall in turn affects macrophage gene expression and SMC proliferation.[18] Histopathological studies have shown the localization of matrix metalloproteinase (MMP)-1 in regions of high circumferential strain within plaques, suggesting that viscoelastic properties influence MMP release, further weakening plaque structure contributing to a greater tendency toward plaque rupture.[19] Plaque instability is influenced by the proteolysis of fibrous cap collagen by MMPs released by activated macrophages and apoptosis of vascular

Address all correspondence to: Seemantini K. Nadkarni, Massachusetts General Hospital, Harvard Medical School, Wellman Center for Photomedicine, Boston, Massachusetts 02114. Tel: (617)-724-1381; Fax: (617)-7264103; E-mail: snadkarni@mgh.harvard.edu

smooth muscle cells (VSMCs), which impede collagen synthesis, further weakening the fibrous cap.[20–22] Finite element analysis (FEA) studies of coronary cross-sections derived from histology sections, or IVUS and OCT images, show that peak stresses associated with plaque rupture critically depend on the geometry and viscoelastic properties of the fibrous cap and lipid pool, and plaque rupture becomes imminent when the peak stress in the plaque surpasses a critical threshold.[23–25] The final event of plaque rupture is therefore a biomechanical failure that occurs when a plaque with severely compromised mechanical properties is unable to withstand loads exerted on it.[23,24,26–33]

Thus, there is much supporting evidence that mechanical factors both regulate and influence all aspects of atherosclerosis development in arteries from lesion initiation to plaque rupture, enforcing the need for novel approaches for measuring biomechanical markers to obtain insights on disease etiology and predict the risk of acute events. Optical approaches offer new opportunities for the evaluation of the constitutive mechanical properties of the arterial wall. The attractive characteristics of optical modalities are that they are nondestructive; they may be combined with other techniques to allow simultaneous measurements of multiple microstructural, molecular, and mechanical features; and they are amenable to implementation using flexible small-diameter fiber-optic catheters for *in vivo* use. In this paper, we review multiple mechanical factors that play a role in plaque initiation, progression, and rupture, and provide a critical overview of current optical approaches to investigate biomechanical factors involved in various stages of atherosclerosis development.

2 Influence of Extracellular Matrix and Cell Mechanical Properties on Plaque Initiation and Progression

In the early stages of lesion initiation, cellular, molecular, and compositional factors modulate the mechanical properties of the arterial wall.[34–36] Recent studies indicate that these mechanical alterations are not merely a result of disease pathogenesis, but may in fact actively drive cell signaling and regulate atherogenesis and vascular disease progression.[37] In particular, the uncontrolled proliferation and migration of VSMCs accompanied by increased ECM deposition influence early lesion initiation as well as the development of coronary occlusive disease.[38–41] Increased ECM stiffness regulates cell adhesion, proliferation, and migration, and VSMC behavior may be modified by modulating substrate mechanical properties.[42–47] Adherent mammalian cells feel, perceive, and respond to the mechanical properties of their substrate through transmembrane integrin receptors,[48–51] and changes in ECM stiffness may influence cellular responses to growth factors via a cooperative dialogue between integrin and growth factor receptor signaling pathways.[52,53] The platelet-derived growth factor (PDGF) in particular is a major stimulus for VSMC migration and proliferation. Brown et al. recently showed that increased substrate stiffness enhances PDGF receptor activity, abnormal VSMC proliferation, and increased integrin signaling, which in turn modulates cell elasticity.[42] Peyton and Putnam showed that increased ECM rigidity regulates cytoskeleton assembly and cell migration speed, and that VSMCs on stiffer substrates demonstrated an increase in the number and size of focal adhesions, paralleled with an increased F-actin stress fiber formation and enhanced cell stiffness.[46] Endothelial cell (EC) dysfunction is a key step in the pathogenesis of atherosclerosis in the vessel wall. EC micromechanical factors including cell mechanical properties, deformability, and cell–cell communication play a major role in EC function.[54–57] Shentu et al. showed that exposure to oxidized low-density lipoprotein (oxLDL) increases EC rigidity and that cell elastic modulus increased linearly with the progressive oxidation of LDL.[54,58] Studies also showed that ECs isolated from hypercholesterolemic pigs were significantly stiffer than normo-cholesterolemic controls, further suggesting an association among EC micromechanics, endothelial dysfunction, and lipid exposure.[56] The adhesion of monocytes to arterial ECs and their migration into the intima are the earliest events in atherosclerotic lesion initiation. Kataoka et al. showed that the elastic modulus of ECs decreased following monocyte adhesion, which subsequently reduced the adhesiveness of ECs to the vessel wall and increased the deformability of ECs, potentially facilitating monocyte migration into the intima.[59] These observations suggest that the pathogenesis of atherosclerosis is driven by a cooperative dialogue between ECM mechanics and cell signaling, underscoring the fact that knowledge of the mechanical properties of the ECM and vascular cells is crucial in advancing our understanding of atherosclerosis etiology, and developing new therapies and prognostic indicators to manage atherosclerosis at early stages of the disease.

3 Optical Tools to Measure the Mechanical Properties of Vascular Cells and ECM Components

A number of approaches have been implemented for measuring the mechanical properties of living cells and ECM protein constituents. Some of these approaches include atomic force microscopy, traction force microscopy (TFM), subcellular laser ablation, micropost arrays, active and passive microrheology approaches, and MEMS-based devices. Here, we explore two promising optical approaches, optical microrheology and TFM, that have been applied to investigate the mechanical properties of arterial ECM components and live ECs and VSMCs.

3.1 *Optical Microrheology*

Passive optical microrheology, a technique introduced in 1995 by Mason and Weitz, probes the local viscoelastic properties of a medium by measuring the thermal or passive Brownian displacements of probe particles.[60] In conventional rheometry, the viscoelastic or complex modulus is calculated by measuring the mechanical strain in a material in response to an external stress. In contrast, in optical microrheology, the mean square displacement (MSD) of tracer probes or endogenous particles is quantified using video microscopy or dynamic light scattering techniques, and the estimated MSD is related with the complex frequency-dependent viscoelastic modulus, G*, via the generalized Stokes–Einstein relation.[61–63] Over the past decade, microrheology approaches have been extended to biological systems to measure the viscoelastic moduli of living cells, subcellular components, and ECM proteins using synthetic[64–66] or endogenous light scattering particles[66] as well as fluorescently labeled nano- and microbeads as tracer probes.[67,68] In particle tracking microrheology, micron-sized fluorescent beads are injected within a living cell and passive bead displacements are subsequently tracked using a fluorescence microscope and a high-frame-rate camera to measure the mechanical compliance of the cytoplasm over time scales of 0.1 to 10 s (Fig. 1).[69,70]

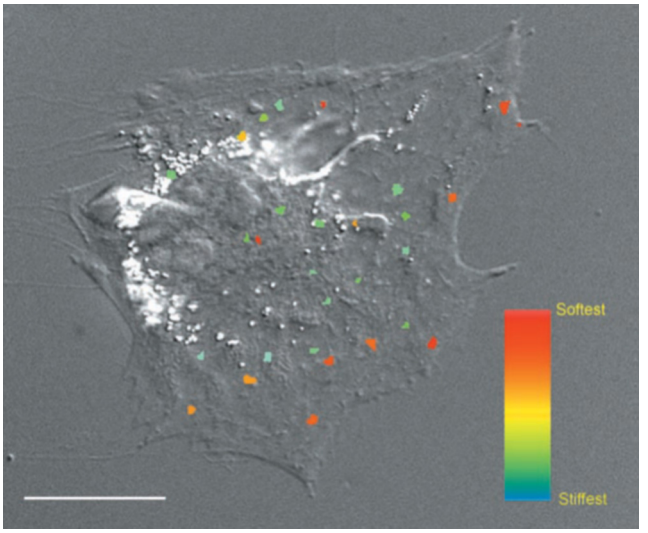

Fig. 1 Multiple-particle microrheology to map the compliance of the cytoplasm in a living endothelial cell. A differential interference contrast (DIC) image was superimposed to a fluorescence image of the trajectories of injected tracer microspheres. Tracer trajectories, recorded for 20 s, were transformed into local compliances, which were normalized by the maximum compliance. The color represents compliance between red (most compliant microenvironment within the cell) to blue (least compliant microenvironment). Scale bar, 30 μm. Reprinted from Tseng et al.[70]

Using this approach, studies have shown that ECs display directional mechanical anisotropy modulated by fluid shear stress (Fig. 2),[64] that endothelial growth factors responsible for EC migration modulate the mechanical properties of the EC cytoplasm in three-dimensional matrices,[65] and that the introduction of inflammatory agents causes a rapid stiffening of ECs.[71] In another approach, viscoelastic properties are estimated by implementing dynamic light scattering formalisms to measure rapid time-resolved intensity fluctuations of backscattered light or laser speckle detected following single or multiple light scattering and diffusion through tissue.[60,61,72,73] Because speckle fluctuations are sensitive to subwavelength-scale thermal displacements, this approach allows measurement over an extended dynamic range of viscoelastic moduli from 0.1 Pa to 10 kPa over a frequency range of 1 Hz to 1 kHz[72] and therefore may be better suited for evaluating stiffer ECM components and synthetic cell substrates compared to particle tracking microscopy approaches.[61,72] An improved frequency range can be obtained using a new technique termed fast fluorescence laser tracing microrheology, which incorporates high-sensitivity fluorescence detection electronics to enable nanometer-scale spatial resolution over a large frequency range of 1 Hz to 50 kHz.[74,75] In addition to the passive microrheology approaches explored above, the displacement of tracer beads can be actively driven to probe the mechanical properties of the local microenvironment using magnetic and laser tweezers. In particular, magnetically actuated microrheology techniques have been used to probe the elastic properties of the transmembrane receptors in vascular ECs and ECM proteins by binding functionalized magnetic nanoparticles and subsequently measuring displacement fields.[71,76] Active measurements allow the possibility of applying large stresses greater than the intrinsic thermal energy required to modulate the trajectory of probe particles and therefore allow the possibility of characterizing stiffer vascular ECMs over a larger range of viscoelastic moduli compared to passive microrheology approaches. The requirement for the use of extrinsic probe particles for active microrheology approaches and the difficulty in achieving uniform beam distribution, however, restrict these measurements to the local bead microenvironment. In contrast, passive microrheology approaches offer the potential to evaluate local mechanical properties by quantifying the trajectories of light scattering particles intrinsic within tissue without the need for external probe particles, albeit over a smaller dynamic range of viscoelastic moduli compared with active approaches.[72,73] In these cases, however, technical considerations to accurately estimate the particle size distribution[77–79] of intrinsic light scatterers and the influence of sample optical properties on passive microrheology results are yet to be completely addressed.[66]

3.2 *Traction Force Microscopy*

In contrast to optical microrheology-based approaches, in which cell and ECM mechanical properties are directly estimated from the passive motion or active manipulation of probe particles, TFM measures contractile tension or traction forces exerted by cells against the substrate.[80] Cells generate traction forces on their local ECM microenvironment via focal adhesion complexes during cell adhesion and migration, and traction forces are relayed to the cell nucleus via transmembrane mechanotransduction proteins involved in sensing substrate stiffness. It is clear that ECM stiffness is directly linked with the extent of tension generated at focal adhesion sites; therefore, by measuring cell traction forces, TFM may probe the mechanical properties of the local ECM microenvironment.[81–83] In a TFM experiment, cells are cultured on an optically clear polyacrylamide substrate coated with ECM constituents, and the motion of fluorescent fiduciary microbeads embedded within the gel is tracked. Traction forces are then determined by analyzing bead displacements during cell migration via the digital cross-correlation of images obtained during adhesion (stressed state) and following detachment (unstressed state) (Fig. 3).[83,84] Traction forces are then calculated from the bead displacement vector field

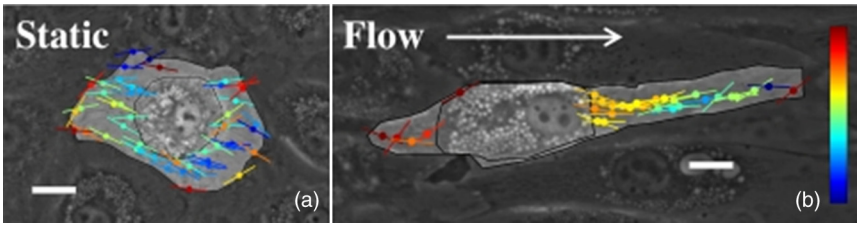

Fig. 2 Magnitude and directionality of creep compliance within vascular endothelial cells. (a) Before application of laminar flow shear stress (LSS). (b) Twenty-four hours after starting LSS. Circles indicate the average position of each tracked marker. Hot and cold colors indicate, respectively, low and high creep compliance. Reprinted from del Alamo et al.[64]

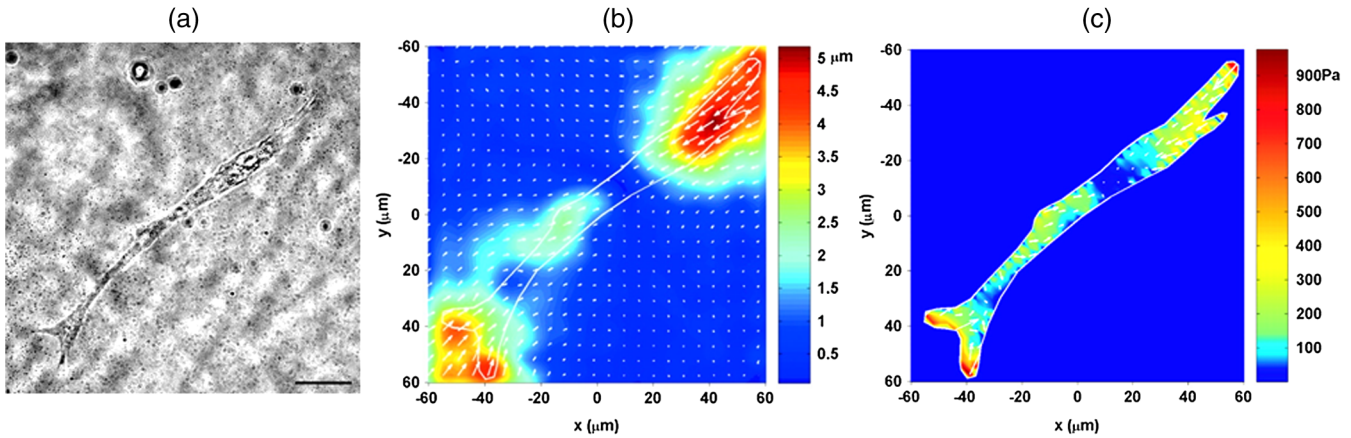

Fig. 3 Traction force microscopy of smooth muscle cells. (a) Phase image of a smooth muscle cell cultured on the polyacrylamide gel coated with collagen type I (Bar, 20 μm). (b) The displacement vector field computed from the two fluorescent images of the 0.2-μm diameter tracer microbeads in the gel (images are obtained 3 min apart during cell attachment and detachment from the substrate). Arrows show the direction and magnitude of the displacement field of the gel under the cell. Colors show the absolute magnitude of the displacements in micrometers. (c) The traction field computed from the displacement field shown in (b). Arrows show the direction and relative magnitude of the tractions. Colors show the magnitude of the traction vectors in Pa. Reprinted from Wang and Lin.[80]

by solving the inverse problem using a variety of approaches, which include the generation of a quadrilateral mesh to evaluate the traction field[85] or a more computationally efficient fast Fourier transform-based algorithm that recasts the relationship between bead displacements and traction into Fourier space to recover the traction field.[83] TFM has been used to measure traction forces in a variety of arterial cell types to evaluate EC cell-cell contacts,[86] to understand the modulation of EC behavior and function in response to ECM stiffening,[82] and to evaluate the tensile properties of stress fibers in VSMCs.[87] With the increasing spatial resolution of TFM tools, it is now possible to measure traction forces generated by individual, micron-sized focal adhesions to evaluate spatial differences within the traction force field at the leading and trailing edges of a single living cell.[88] Recently, TFM has been extended to measure cell-induced three-dimensional traction fields by tracking the motion of submicron fluorescent markers using laser scanning confocal microscopy and digital volume correlation.[89]

4 Role of Arterial Mechanical Properties in Mediating Plaque Rupture

In advanced stages of atherosclerosis, the rupture of the fibrous cap is recognized as the trigger event for AMI, and pathologic analyses of ruptured fibrous caps have demonstrated that 95% of ruptured caps were <65 μm in thickness.[1,2] Early biomechanical analyses using finite element analysis (FEA) techniques showed that thin fibrous caps are predisposed to rupture at a peak stress threshold >300 kPa.[23,35] More recent studies, however, challenge the <65 μm cap thickness criterion, indicating that caps >100 μm often rupture at stress levels far lower than the 300-kPa threshold.[90–92] The inability to explain plaque rupture in thick caps has prompted a number of FEA studies to test other biomechanical factors of cap rupture that include necrotic core composition, thickness and angle,[16,24,25,93] residual stress distribution,[94] and the presence and location of microcalcifications in the fibrous cap.[90] Collectively, these studies showed that (1) the presence of a large necrotic core elevated peak cap stress and increased the risk of rupture,[25] (2) cholesterol constituents of the lipid pool modulated peak stress distribution,[16] (3) residual stress influenced the extent and location of peak stress, and (4) peak stress could be elevated by fivefold in the presence of microcalcifications.[95,96] Using idealized model geometries, a recent study showed that peak stress was increased in fibrous caps with intermediate and elevated elastic moduli, and for softer fibrous caps, the necrotic core thickness and necrotic core angle had greater impact on the peak cap stress.[97] Loree et al. demonstrated that mechanical properties of the lipid pool are influenced by cholesterol, phospholipids, and triglyceride content, and the concentration of these lipid constituents may affect cap stress distribution.[16] Thus, based on simulation results, the measurement of peak stress is recognized as a good biomechanical predictor of plaque rupture. The key challenge is that mechanical stress predictions using FEA techniques critically depend on accurate estimates of the mechanical properties of the necrotic core, fibrous cap, and other plaque constituents. Unfortunately, this information is not readily available, and current knowledge of plaque mechanical properties has been limited to tensile and compression testing of cadaveric and animal arteries conducted *ex vivo*. Due to the dearth of tools to measure arterial mechanical properties *in vivo* and the heterogeneity of advanced coronary plaques at any given stage of plaque growth and remodeling, the precise prediction of peak stress in coronary vessels of patients remains challenging.

5 Intravascular Optical Tools to Measure the Mechanical Properties of Coronary Plaques

IVUS elastography is currently the only clinically available tool to assess the mechanical properties of fibrous caps and lipid pools. However, given the low spatial resolution of IVUS elastography (~1 mm), this technique is yet incapable of evaluating the mechanical properties of thin fibrous caps that are implicated in the majority of acute coronary events. Optical imaging approaches hold the potential of providing superior spatial resolution for the mechanical analysis of TCFA lesions. We explore three promising optical imaging modalities, laser speckle rheology (LSR), optical coherence elastography, and polarization-sensitive (PS) OCT, which have been under development over many years and have recently undergone significant technical improvements to enable intracoronary assessment as outlined below.

5.1 *Laser Speckle Rheology*

LSR measures the mechanical properties of atherosclerotic plaques by evaluating the time-scale of intensity fluctuations from time-varying laser speckle patterns (Fig. 4).[73] When a scattering medium such as tissue is imaged using temporally coherent light from a laser, a granular speckle pattern becomes apparent as a result of multiple scattering and interference of photons returning from different regions within the tissue. In tissue, the Brownian motion of endogenous light scattering particles causes scatter locations and optical path lengths to dynamically change, resulting in time-dependent intensity modulations of the detected laser speckle patterns.[60,61] As described above, the rate of laser speckle modulation is highly dependent on the motion of endogenous scatterers, which is in turn influenced by the viscoelasticity of the medium.[66,72,73,98] Using these principles, a study conducted on *ex vivo* arteries has demonstrated that the measurement of the speckle decorrelation time constant of intensity modulations of time-varying laser speckle patterns provides an index of plaque viscoelastic properties and enables the mechanical characterization of unstable TCFA lesions with a sensitivity of 100% and a specificity of 93%.[73] By combining the analysis of spatial and temporal information from laser speckle patterns, it has been demonstrated that LSR may additionally provide a measure of plaque fibrous cap thickness.[98] A recent study has shown that LSR can be conducted through small-diameter optical fiber bundles, allowing the opportunity to conduct intracoronary LSR through miniaturized intravascular catheters.[99,100] Low-cross-talk optical fiber bundles with small fiber cores and large core-core spacing (>7 μm) in particular have been shown to permit the robust transmission of laser speckle patterns and enable plaque characterization even during physiological cardiac motion conditions.[99] Recent studies have demonstrated the capability of intracoronary LSR to assess the mechanical properties of native and atherosclerotic arteries in living rabbits[100] and xenograft swine in conjunction with intracoronary balloon occlusion and saline flushing. At present, a clinically viable LSR system has yet to be tested, although active development and preclinical testing in animals is currently ongoing.[100] If successfully translated into the clinical realm, the intracoronary LSR technique will offer the unique possibility of obtaining a direct estimate of the mechanical properties of coronary plaques.

5.2 *Intravascular Optical Coherence Elastography*

Intravascular elastography, traditionally based on IVUS imaging, is an established approach to measure arterial biomechanics by estimating local strains within tissue in response to an applied load. Optical coherence elastography (OCE), first demonstrated in 1998 by Schmitt et al.,[101] takes advantage of the superior resolution and microstructural imaging capabilities of OCT (<10 μm axial and ~20 μm lateral resolution) and holds substantial promise for the detailed characterization of the elastic properties of coronary plaque components.[102] Over the past decade, OCE has been used for high-resolution elasticity imaging in a variety of applications to assess the mechanical properties of the myocardium in a developing embryonic heart,[103] to improve the localization and detection of tumors and tumor boundaries,[104–107] to measure strain maps in corneal tissue,[108] ocular tissues, and human skin,[109,110] and to evaluate lung mechanics in cystic fibrosis.[111] Here, we focus our review on OCE efforts for strain assessment in the arterial wall to enable plaque mechanical characterization and the estimation of plaque elastic properties.[112–114] Traditionally, the majority of OCE methods have measured strain fields by employing speckle tracking strategies based on the two-dimensional cross-correlation of subsequent OCT frames obtained at baseline and following the application of a known load. In the context of intracoronary applications, due to the effects of cardiac motion, catheter rotation during imaging, and high cyclic strains during vessel pulsation, traditional cross-correlation-based OCE methods suffer from unreliable speckle correlations between frames, and the measurement of arterial strain fields is rendered intractable. To address these challenges, Chan et al. introduced a variational framework that exploits *a priori* predictions about arterial wall mechanical behavior to measure robust estimates of tissue velocity and strain, thereby reducing the sensitivity of conventional speckle tracking to both motion and strain-induced speckle intensity decorrelation.[113] Khalil et al. later introduced an improved nonlinear least-squares method that minimized differences between computed and measured deformation to estimate soft-tissue elasticity and resolve heterogeneous inclusions of 100-μm diameter.[112] To further improve the motion tolerance of OCE, van Soest et al. proposed a method termed alternating line elastography in which radial strains in the arterial wall were estimated by optimizing the cross-correlation

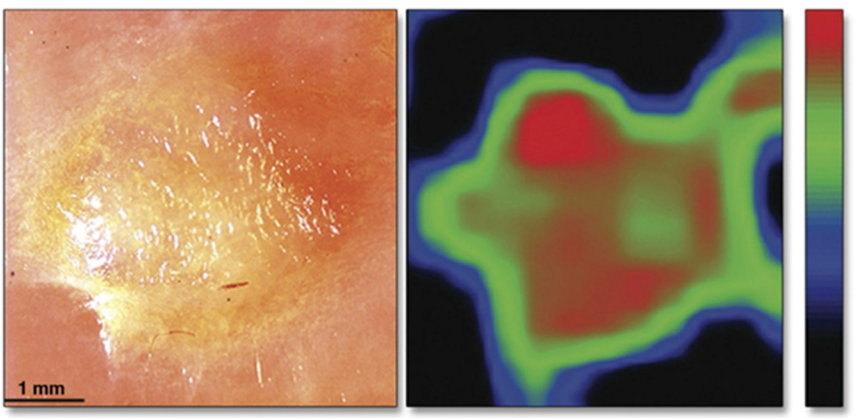

Fig. 4 Laser speckle rheology of atherosclerotic plaques. (a) Gross pathology photograph of a lipid-rich plaque. (b) The corresponding spatial distribution map of the speckle decorrelation time constants related to the viscoelastic properties of the atheroma (scale: black = 400 ms corresponding to stiffer fibrous regions, red = 30 ms corresponding to low-viscosity lipid regions). The plaque borders are clearly visualized in the speckle decorrelation map in addition to regions that correspond to lipid-rich regions of low viscosity. Reprinted from Nadkarni et al.[73]

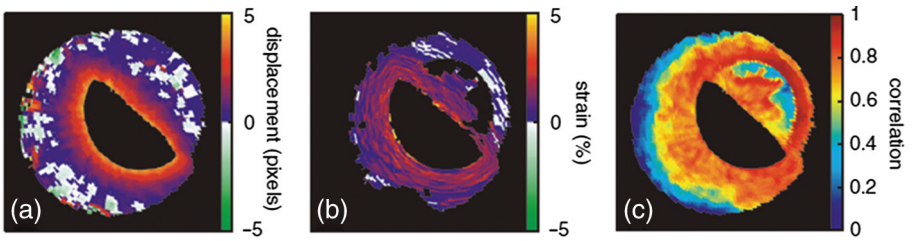

Fig. 5 Optical coherence elastography using alternating A-line correlations. Displacement (a) and strain (b) fields resulting from the alternating line elastography algorithm, and the value of the correlation coefficient (c). Reprinted from van Soest et al.[121]

between two sets of lines (Fig. 5).[115] Because adjacent A-lines are correlated due to overlapping point spread functions in OCT, this method demonstrated reduced sensitivity to motion artifacts and nonuniform catheter rotation. With new improvements in next-generation OCT technology, such as spectral and Fourier domain OCT, recent advances in dynamic OCE have been introduced that circumvent the need for traditional cross-correlation-based speckle tracking.[116] In dynamic OCE, acoustic radiative forces[117,118] or oscillating magnetic fields[119] are applied to drive mechanical perturbations and the local elasticity of tissue is assessed from the detected phase-resolved signals.[120] These methods, however, have not yet been demonstrated in arterial tissue, and further development is needed prior to intracoronary investigation to include simultaneous delivery of acoustic pulses, magnetic field excitation, or magnetic nanoparticles *in vivo*.

5.3 *Polarization-Sensitive OCT*

While LSR and OCE provide direct estimates of the mechanical properties of coronary plaque components, PS-OCT is included in this review because it offers a unique opportunity to evaluate the organization of collagen fibers[122,123] of the arterial ECM, intimately linked with the mechanical stability of the fibrous cap. PS-OCT is an extension to OCT technology that quantifies tissue birefringence, a property that alters the polarization of light and is correlated to macromolecular ECM proteins with organized structure, such as collagen and elastin within fibrous caps. In 2007, a quantitative study examined the utility of PS-OCT to measure collagen birefringence in aortic plaques.[124] The study revealed that increased PS-OCT birefringence correlated with abundant thick collagen fibers and/or the presence of intimal SMC, suggesting that the detection of high birefringence in PS-OCT images implies increased mechanical stability (Fig. 6). Additional *ex vivo* studies have reported the potential of PS-OCT for the assessment of plaque collagen organization[125] and for improving the plaque characterization capability of OCT.[126] While *ex vivo* imaging results using PS-OCT have been promising, the translation of intravascular PS-OCT to the clinical setting for evaluating coronary arteries in patients has been confounded by technical challenges, specifically the wavelength-dependent polarization change introduced by components of the optical system, termed polarization mode dispersion (PMD). For microscope-type OCT systems that do not use rotating catheters, PMD can be avoided by controlling the polarization state of light throughout the system.[127,128] In an intracoronary system that uses a rapidly rotating catheter, however, the polarization state of light cannot be similarly controlled, and polarimetry noise arising from PMD overwhelms the birefringence signal that we seek to measure. Recently, however, a number of solutions to this dilemma have been introduced to mitigate PMD during intracoronary imaging (Fig. 7),[129,130] and *in vivo* studies in animals as well as clinical

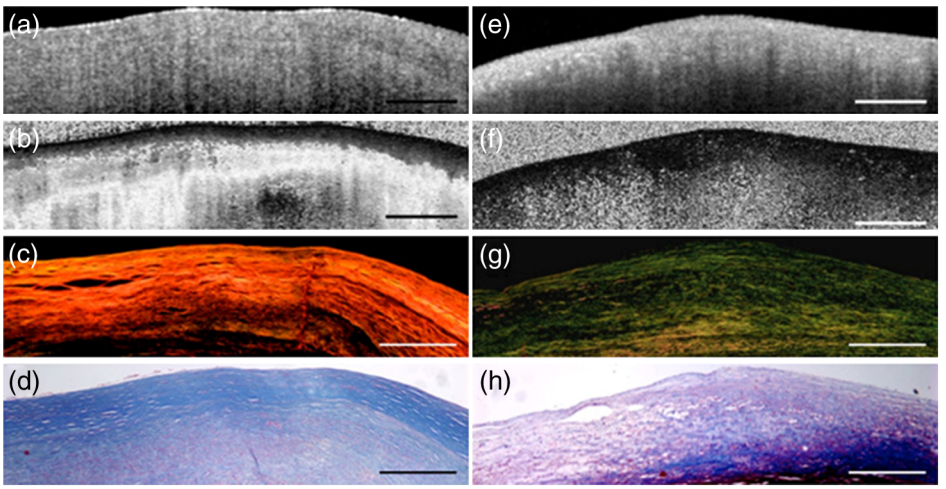

Fig. 6 Polarization-sensitive optical coherence tomography (PS-OCT) images and corresponding histopathology demonstrating collagen birefringence in atherosclerotic plaques. (a) and (e) OCT images of fibrous plaques. (b) PS-OCT image of the fibrous plaque in (a) showing high birefringence as seen by the rapid transition of the image from black to white, corresponding to 0- to 180-deg phase retardation. (c) Picrosirius red-stained histology section showing orange-red fibers (thicker fibers) under polarized light microscopy. (d) and (h) Trichrome stained histology images. (f) PS-OCT image of fibrous plaque showing black region corresponding to low birefringence below the luminal surface. (g) Corresponding picrosirius red–stained histology section showing yellow-green fibers (thinner fibers) under polarized light microscopy. Scale bars = 500 μm. Reprinted from Nadkarni et al.[124]

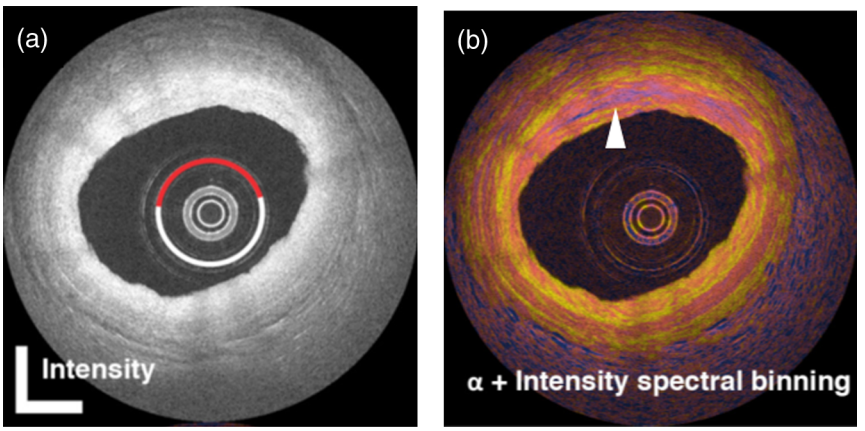

Fig. 7 PS imaging of cadaveric human coronary artery. (a) Intensity image, indicating a region of intimal hyperplasia (white arc of a circle) and a fibrous plaque (red arc of a circle). (b) Local birefringence image obtained using a spectral binning algorithm to mitigate polarization mode dispersion. The arrow points to regions of increased birefringence, suggesting the presence of well-organized collagen. A high-birefringence layer of a vascular smooth muscle cells rich media is clearly visible. Reprinted from Villiger et al.[130]

studies in patients are currently underway. If successful, PS-optical frequency domain imaging (OFDI) may prove to be a powerful approach in our arsenal of intravascular optical imaging technologies to measure mechanical alterations of the fibrous cap that may occur as a result of collagen disorganization.

6 Implications and Future Directions

Mechanical factors are implicated in every stage of atherosclerosis progression from lesion initiation to plaque rupture. In early lesions, among other factors, the pathogenesis of atherosclerosis is likely mediated by a synergistic dialogue between the ECM and cell mechanical cues and intracellular signaling. Therefore, knowledge of the mechanical properties of living cells and their ECM microenvironment obtained using techniques such as optical microrheology and TFM will likely advance current understanding of the etiology of atherosclerosis for developing new rheology-informed diagnostic and therapeutic approaches to manage the early stages of disease progression.

In advanced coronary lesions, the intracoronary assessment of plaque mechanical properties will likely play a role in implementing new paradigms for the detection of vulnerable plaques in patients at risk for AMI. The detection of vulnerable plaque has remained a holy grail in the field of interventional cardiology over many years. While intravascular methods, including OCT, OFDI, VH-IVUS, and NIRS, have been developed to visualize various features of vulnerable plaques, there is yet no single technique that has unequivocally demonstrated the capability to accurately predict plaque rupture in patients. This is because plaque rupture leading to coronary thrombosis is a complex, multifactorial problem that involves multiple compositional, hemodynamic, microstructural, and inflammatory parameters that act in tandem to alter the mechanical fragility of the plaque. As a result, the final event of plaque rupture results from the failure of a mechanically compromised plaque. The intravascular laser speckle rheology (ILSR), OCE, and PS-OCT technologies outlined here elegantly lend themselves for integration with other intracoronary technologies such as OCT and IVUS that could place direct mechanical findings within a morphologic context for a composite evaluation of coronary plaque stability to predict the propensity of plaque rupture. These approaches, however, are currently in their early stages of clinical development and implementation, and have not yet demonstrated clinical evidence to predict plaque vulnerability in patients. Yet, they are currently the only techniques available that offer the unique opportunity to detect mechanically compromised plaques and therefore warrant further investigation. Furthermore, biomechanical analysis and clinical studies have shown that volumetric imaging of plaque architecture in three dimensions provides important insights on plaque stability that are not fully appreciated by viewing individual tomograms. Therefore, in the future, methods to measure and map plaque mechanical properties in three dimensions will require further development and implementation to sufficiently advance our understanding of plaque rupture and coronary thrombotic complications in patients.

References

1. R. Virmani et al., "Vulnerable plaque: the pathology of unstable coronary lesions," *J. Interv. Cardiol* **15**, 439–446 (2002).
2. R. Virmani et al., "Lessons from sudden coronary death: a comprehensive morphological classification scheme for atherosclerotic lesions," *Arterioscler. Thromb. Vasc. Biol.* **20**(5), 1262–1275 (2000).
3. G. J. Tearney et al., "Three-dimensional coronary artery microscopy by intracoronary optical frequency domain imaging," *JACC Cardiovasc. Imaging* **1**, 752–761 (2008).
4. P. R. Moreno et al., "Detection of lipid pool, thin fibrous cap, and inflammatory cells in human aortic atherosclerotic plaques by near-infrared spectroscopy," *Circulation* **105**(8), 923–927 (2002).
5. Y. Uchida et al., "Percutaneous coronary angioscopy," *Jpn. Heart J.* **33**(3), 271–294 (1992).
6. A. V. Finn et al., "Concept of vulnerable/unstable plaque," *Atheroscler. Throm. Vasc. Biol.* **30**, 1282–1292 (2010).
7. E. Arbustini et al., "Coronary atherosclerotic plaques with and without thrombus in ischemic heart syndromes: a morphologic, immunohistochemical and biochemical study," *Am. J. Cardiol.* **68**, 36B–50B (1991).
8. P. K. Cheruvu et al., "Frequency and distribution of thin-cap fibroatheroma and ruptured plaques in human coronary arteries," *J. Am. Coll. Cardiol.* **50**(10), 940–949 (2007).
9. P. W. Serruys, H. M. Garcia-Garcia, and E. Regar, "From postmortem characterization to the *in vivo* detection of thin capped fibroatheromas: the missing link towards percutaneous treatment," *J. Am. Coll. Cardiol.* **50**(10), 950–952 (2007).
10. G. W. Stone et al., "A prospective natural-history study of coronary atherosclerosis," *N. Engl. J. Med.* **364**(3), 226–235 (2009).
11. M. Mizukoshi et al., "Clinical classification and plaque morphology determined by optical coherence tomography in unstable angina pectoris," *Am. J. Cardiol.* **106**(3), 323–328 (2010).

12. A. Tanaka et al., "Lipid rich plaque and myocardial perfusion after successful stenting in patients with non-st segment elevation acure coronary syndrome: an optical coherence tomography study," *Eur. Heart J.* **30**(11), 1348–1355 (2009).
13. K. Koskinas et al., "Natural history of experimental coronary atherosclerosis and vascular remodeling in relation to endothelial shear stress: a serial, *in vivo* intravascular ultrasound study," *Circulation* **121**(19), 2092–2101 (2010).
14. M. Papafaklis et al., "*In-vivo* assessment of the natural history of coronary atherosclerosis: vascular remodeling and endothelial shear stress determine the complexity of atherosclerotic disease progression," *Curr. Opin. Cardiol.* **25**(6), 627–638 (2010).
15. F. Kolodgie et al., "Free cholesterol in atherosclerotic plaques: where does it come from?," *Curr. Opin. Lipidol.* **18**(5), 500–507 (2007).
16. H. M. Loree et al., "Mechanical properties of model atherosclerotic lesion lipid pools," *Arterioscler. Thromb.* **14**(2), 230–234 (1994).
17. J. A. Schaar et al., "Characterizing vulnerable plaque features with intravascular elastography," *Circulation* **108**(21), 2636–2641 (2003).
18. R. T. Lee et al., "Mechanical strain induces specific changes in the synthesis and organization of proteoglycans by vascular smooth muscle cells," *J. Biol. Chem.* **276**(17), 13847–13851 (2001).
19. R. T. Lee et al., "Integrin-mediated collagen matrix reorganization by cultured human vascular smooth muscle cells," *Circ. Res.* **76**(2), 209–214 (1995).
20. G. Bauriedel et al., "Role of smooth muscle cell death in advanced coronary primary lesions: implications for plaque instability," *Cardiovasc. Res* **41**(2), 480–488 (1999).
21. A. C. Newby and A. B. Zaltsman, "Fibrous cap formation or destruction—the critical importance of vascular smooth muscle cell proliferation, migration and matrix formation," *Cardiovasc. Res.* **41**(2), 345–360 (1999).
22. M. D. Rekhter et al., "Hypercholesterolemia causes mechanical weakening of rabbit atheroma: local collagen loss as a prerequisite of plaque rupture," *Circ. Res.* **86**(1), 101–108 (2000).
23. P. D. Richardson, M. J. Davies, and G. V. Born, "Influence of plaque configuration and stress distribution on fissuring of coronary atherosclerotic plaques," *Lancet* **2**(8669), 941–944 (1989).
24. G. Finet, J. Ohayon, and G. Rioufol, "Biomechanical interaction between cap thickness, lipid core composition and blood pressure in vulnerable coronary plaque: impact on stability or instability," *Coron. Artery Dis.* **15**(1), 13–20 (2004).
25. J. Ohayon et al., "Necrotic core thickness and positive arterial remodelling index: emergent biomechanical factors for evaluating the risk of plaque rupture," *Am. J. Physiol. Heart Circ. Physiol* **295**, H717–H727 (2008).
26. R. Lee, "Atherosclerotic lesion mechanics versus biology," *Z Kardiol* **89**(2), 80–84 (2000).
27. S. D. Williamson et al., "On the sensitivity of wall stresses in diseased arteries to variable material properties," *J. Biomech. Eng.* **125**, 147–155 (2003).
28. P. K. Shah, "Mechanisms of plaque vulnerability and rupture," *J. Am. Coll. Cardiol.* **41**, 15S–22S (2003).
29. L. Arroyo and R. Lee, "Mechanisms of plaque rupture: mechanical and biologic interactions," *Cardiovasc. Res.* **41**(2), 369–375 (1999).
30. P. D. Richardson, "Biomechanics of plaque rupture: progress, problems, and new frontiers," *Ann. Biomed. Eng.* **30**(4), 524–536 (2002).
31. G. Finet et al., "Morphological and biomechanical aspects of vulnerable coronary plaque," *Arch Mal Coeur Vaiss* **100**(6–7), 547–553 (2007).
32. J. Ohayon et al., "Influence of residual stress/strain on the biomechanical stability of vulnerable coronary plaques: potential impact for evaluating the risk of plaque rupture," *Am. J. Physiol. Heart Circ. Physiol.* **293**(3), H1987–1996 (2007).
33. U. Sadat, Z. Teng, and J. H. Gillard, "Biomechanical structural stresses of the atherosclerotic plaque," *Expert Rev. Cardiovasc Ther.* **8**(10), 1469–1481 (2010).
34. J. G. Jacot et al., "Early adaptation of human lower extremity vein grafts: wall stiffness changes accompany geometric remodeling," *J. Vasc. Surg.* **39**(3), 547–555 (2004).
35. R. T. Lee et al., "Structure-dependent dynamic mechanical behavior of fibrous caps from human atherosclerotic plaques," *Circulation* **83**(5), 1764–1770 (1991).
36. T. Matsumoto et al., "Local elastic modulus of atherosclerotic lesions of rabbit thoracic aortas measured by pipette aspiration method," *Physiol. Meas.* **23**(4), 635–648 (2002).
37. D. E. Ingber, "Mechanobiology and diseases of mechanotransduction," *Ann. Med.* **35**(8), 564–577 (2003).
38. K. Imanaka-Yoshida et al., "Serial extracellular matrix changes in neointimal lesions of human coronary artery after percutaneous transluminal coronary angioplasty: clinical significance of early tenascin-c expression," *Virchows Arch.* **439**(2), 185–190 (2001).
39. S. T. Nikkari et al., "Smooth muscle cell expression of extracellular matrix genes after arterial injury," *Am. J. Pathol.* **144**(6), 1348–1356 (1994).
40. J. Thyberg, "Phenotypic modulation of smooth muscle cells during formation of neointimal thickenings following vascular injury," *Histol. Histopathol.* **13**(3), 871–891 (1998).
41. J. Thyberg et al., "Phenotypic modulation of smooth muscle cells after arterial injury is associated with changes in the distribution of laminin and fibronectin," *J. Histochem. Cytochem.* **45**(6), 837–846 (1997).
42. X. Q. Brown et al., "Effect of substrate stiffness and pdgf on the behavior of vascular smooth muscle cells: implications for atherosclerosis," *J. Cell Physiol.* **225**(1), 115–122 (2010).
43. A. Engler et al., "Substrate compliance versus ligand density in cell on gel responses," *Biophys. J.* **86**(1 Pt 1), 617–628 (2004).
44. B. C. Isenberg et al., "Vascular smooth muscle cell durotaxis depends on substrate stiffness gradient strength," *Biophys. J.* **97**(5), 1313–1322 (2009).
45. D. P. McDaniel et al., "The stiffness of collagen fibrils influences vascular smooth muscle cell phenotype," *Biophys. J.* **92**(5), 1759–1769 (2007).
46. S. R. Peyton and A. J. Putnam, "Extracellular matrix rigidity governs smooth muscle cell motility in a biphasic fashion," *J. Cell Physiol.* **204**(1), 198–209 (2005).
47. J. Y. V. Wong et al., "Movement of vascular smooth muscle cells on gradient-compliant hydrogels," *Langmuir* **19**(5), 1908–1913 (2003).
48. D. E. Ingber, "Mechanosensation through integrins: cells act locally but think globally," *Proc. Natl. Acad. Sci. U. S. A.* **100**(4), 1472–1474 (2003).
49. A. Katsumi et al., "Integrins in mechanotransduction," *J. Biol. Chem.* **279**(13), 12001–12004 (2003).
50. M. J. Paszek et al., "Tensional homeostasis and the malignant phenotype," *Cancer Cell* **8**, 241–254 (2005).
51. H. B. Wang et al., "Focal adhesion kinase is involved in mechanosensing during fibroblast migration," *Proc. Natl. Acad. Sci. U. S. A.* **98**(20), 11295–11300 (2001).
52. J. W. Lee and R. Juliano, "Mitogenic signal transduction by integrin- and growth factor receptor-mediated pathways," *Mol. Cells* **17**(2), 188–202 (2004).
53. C. K. Miranti and J. S. Brugge, "Sensing the environment: a historical perspective on integrin signal transduction," *Nat. Cell Biol.* **4**(4), E83–90 (2002).
54. T. P. Shentu et al., "The role of oxysterols in control of endothelial stiffness," *J. Lipid Res.* **53**(7), 1348–1358 (2012).
55. G. B. Kowalsky, F. J. Byfield, and I. Levitan, "oxLDL facilitates flow-induced realignment of aortic endothelial cells," *Am. J. Physiol. Cell Physiol.* **295**(2), C332–340 (2008).
56. F. J. Byfield et al., "oxLDL increases endothelial stiffness, force generation, and network formation," *J. Lipid Res.* **47**(4), 715–723 (2006).
57. H. Oberleithner et al., "Plasma sodium stiffens vascular endothelium and reduces nitric oxide release," *Proc. Natl. Acad. Sci. U. S. A.* **104**(41), 16281–16286 (2007).
58. T. P. Shentu et al., "oxLDL-induced decrease in lipid order of membrane domains is inversely correlated with endothelial stiffness and network formation," *Am. J. Physiol. Cell Physiol.* **299**(2), C218–229 (2010).
59. N. Kataoka et al., "Measurements of endothelial cell-to-cell and cell-to-substrate gaps and micromechanical properties of endothelial cells during monocyte adhesion," *Proc. Natl. Acad. Sci. U. S. A.* **99**(24), 15638–15643 (2002).
60. T. G. Mason and D. A. Weitz, "Optical measurements of frequency-dependent linear viscoelasticity moduli of complex fluids," *Phys. Rev. Lett.* **74**(7), 1250–1253 (1995).
61. B. R. Dasgupta and D. A. Weitz, "Microrheology of cross-linked polyacrylamide networks," *Phys. Rev. E Stat. Nonlin. Soft Matter Phys.* **71**(2 Pt 1), 021504 (2005).

62. B. R. Dasgupta et al., "Microrheology of polyethylene oxide using diffusing wave spectroscopy and single scattering," *Phys. Rev. E Stat. Nonlin. Soft Matter Phys.* **65**(5 Pt 1), 051505 (2002).
63. S. Yamada, D. Wirtz, and S. C. Kuo, "Mechanics of living cells measured by laser tracking microrheology," *Biophys. J.* **78**, 1736–1747 (2000).
64. J. C. del Alamo et al., "Anisotropic rheology and directional mechanotransduction in vascular endothelial cells," *Proc. Natl. Acad. Sci. U. S. A.* **105**(40), 15411–15416 (2008).
65. P. Panorchan et al., "Microrheology and rock signaling of human endothelial cells embedded in a 3d matrix," *Biophys. J.* **91**(9), 3499–3507 (2006).
66. Z. Hajjarian and S. K. Nadkarni, "Evaluation and correction for optical scattering variations in laser speckle rheology of biological fluids," *PLoS One* **8**(5), e65014 (2013).
67. J. Michaelson et al., "Depth-resolved cellular microrheology using hilo microscopy," *Biomed. Opt. Express* **3**(6), 1241–1255 (2012).
68. S. Rathgeber et al., "Microrheology with fluorescence correlation spectroscopy," *Langmuir* **25**(11), 6368–6376 (2009).
69. D. Wirtz, "Particle-tracking microrheology of living cells: principles and applications," *Annu. Rev. Biophys.* **38**, 301–326 (2009).
70. Y. Tseng, T. P. Kole, and D. Wirtz, "Micromechanical mapping of live cells by multiple-particle-tracking microrheology," *Biophys. J.* **83**(6), 3162–3176 (2002).
71. A. R. Bausch et al., "Rapid stiffening of integrin receptor-actin linkages in endothelial cells stimulated with thrombin: a magnetic bead microrheology study," *Biophys. J.* **80**(6), 2649–2657 (2001).
72. Z. Hajjarian and S. K. Nadkarni, "Evaluating the viscoelastic properties of tissue from laser speckle fluctuations," *Sci. Rep.* **2**, 316 (2012).
73. S. K. Nadkarni et al., "Characterization of atherosclerotic plaques by laser speckle imaging," *Circulation* **112**(6), 885–892 (2005).
74. M. Jonas et al., "Fast fluorescence laser tracking microrheometry. I: Instrument development," *Biophys. J.* **94**(4), 1459–1469 (2008).
75. M. Jonas et al., "Fast fluorescence laser tracking microrheometry. II: Quantitative studies of cytoskeletal mechanotransduction," *Biophys. J.* **95**(2), 895–909 (2008).
76. A. R. Bausch, W. Moller, and E. Sackmann, "Measurement of local viscoelasticity and forces in living cells by magnetic tweezers," *Biophys. J.* **76**(1 Pt 1), 573–579 (1999).
77. A. Wax et al., "Determination of particle size by using the angular distribution of backscattered light as measured with low-coherence interferometry," *J. Opt. Soc. Am. A Opt. Image Sci. Vis.* **19**(4), 737–744 (2002).
78. A. Wax, "Low-coherence light scattering calculations for polydisperse size distributions," *J. Opt. Soc. Am. A Opt. Image Sci. Vis.* **22**(2), 256–261 (2005).
79. J. Pyhtila and A. Wax, "Polarization effects on scatterer sizing accuracy analyzed with frequency-domain angle-resolved low-coherence interferometry," *Appl. Opt.* **46**(10), 1735–1741 (2007).
80. J. H. Wang and J. S. Lin, "Cell traction force and measurement methods," *Biomech. Model. Mechanobiol.* **6**(6), 361–371 (2007).
81. C. M. Kraning-Rush et al., "Quantifying traction stresses in adherent cells," *Methods Cell Biol.* **110**, 139–178 (2012).
82. J. P. Califano and C. A. Reinhart-King, "Substrate stiffness and cell area predict cellular traction stresses in single cells and cells in contact," *Cell. Mol. Bioeng.* **3**(1), 68–75 (2010).
83. J. P. Butler et al., "Traction fields, moments, and strain energy that cells exert on their surroundings" *Am. J. Physiol. Cell Physiol.* **282**(3), C595–605 (2002).
84. S. Sen and S. Kumar, "Combining mechanical and optical approaches to dissect cellular mechanobiology," *J. Biomech.* **43**(1), 45–54 (2010).
85. M. Dembo and Y. L. Wang, "Stresses at the cell-to-substrate interface during locomotion of fibroblasts," *Biophys. J.* **76**(4), 2307–2316 (1999).
86. V. Maruthamuthu et al., "Cell-ecm traction force modulates endogenous tension at cell-cell contacts," *Proc. Natl. Acad. Sci. U. S. A.* **108**(12), 4708–4713 (2011).
87. S. Deguchi, T. Ohashi, and M. Sato, "Tensile properties of single stress fibers isolated from cultured vascular smooth muscle cells," *J. Biomech.* **39**(14), 2603–2610 (2006).
88. K. A. Beningo et al., "Nascent focal adhesions are responsible for the generation of strong propulsive forces in migrating fibroblasts," *J. Cell Biol.* **153**(4), 881–888 (2001).
89. C. Franck et al., "Three-dimensional traction force microscopy: a new tool for quantifying cell-matrix interactions," *PloS One* **6**(3), e17833 (2011).
90. N. Maldonado et al., "A mechanistic analysis of the role of microcalcifications in atherosclerotic plaque stability: potential implications for plaque rupture," *Am. J. Physiol. Heart Circ. Physiol.* **303**(5), H619–628 (2012).
91. A. Tanaka et al., "Morphology of exertion-triggered plaque rupture in patients with acute coronary syndrome: an optical coherence tomography study," *Circulation* **118**(23), 2368–2373 (2008).
92. A. Maehara et al., "Morphologic and angiographic features of coronary plaque rupture detected by intravascular ultrasound," *J. Am. Coll. Cardiol.* **40**(5), 904–910 (2002).
93. D. Tang et al., "Effect of a lipid pool on stress/strain distributions in stenotic arteries: 3-d fluid-structure interactions (fsi) models," *J. Biomech. Eng.* **126**(3), 363–370 (2004).
94. J. Ohayon et al., "Influence of residual stress/strain on the biomechanical stability of vulnerable coronary plaques: potential impact for evaluating the risk of plaque rupture," *Am. J. Physiol. Heart Circ. Physiol.* **293**, H1987–1996 (2007).
95. N. Maldonado et al., "The explosive growth of small voids in vulnerable cap rupture; cavitation and interfacial debonding," *J. Biomech.* **46**(2), 396–401 (2013).
96. A. Kelly-Arnold et al., "Revised microcalcification hypothesis for fibrous cap rupture in human coronary arteries," *Proc. Natl. Acad. Sci. U. S. A.* **110**(26), 10741–10746 (2013).
97. A. C. Akyildiz et al., "Effects of intima stiffness and plaque morphology on peak cap stress," *Biomed. Eng. Online* **10**, 25 (2011).
98. S. K. Nadkarni et al., "Measurement of fibrous cap thickness in atherosclerotic plaques by spatiotemporal analysis of laser speckle images," *J. Biomed. Opt.* **11**(2), 021006 (2006).
99. S. K. Nadkarni et al., "Laser speckle imaging of atherosclerotic plaques through optical fiber bundles," *J. Biomed. Opt.* **13**(5), 054016 (2008).
100. Z. Hajjarian et al., "Intravascular laser speckle imaging catheter for the mechanical evaluation of the arterial wall," *J. Biomed. Opt.* **16**(2), 026005 (2011).
101. J. Schmitt, "OCT elastography: imaging microscopic deformation and strain of tissue," *Opt. Express* **3**(6), 199–211 (1998).
102. C. Sun, B. Standish, and V. X. Yang, "Optical coherence elastography: current status and future applications," *J. Biomed. Opt.* **16**(4), 043001 (2011).
103. P. Li and R. K. Wang, "Optical coherence tomography provides an ability to assess mechanical property of cardiac wall of developing outflow tract in embryonic heart *in vivo*," *J. Biomed. Opt.* **17**(12), 120502 (2012).
104. S. Wang et al., "Noncontact measurement of elasticity for the detection of soft-tissue tumors using phase-sensitive optical coherence tomography combined with a focused air-puff system," *Opt. Lett.* **37**(24), 5184–5186 (2012).
105. X. Liang et al., "Dynamic spectral-domain optical coherence elastography for tissue characterization," *Opt. Express* **18**(13), 14183–14190 (2010).
106. X. Liang et al., "Optical micro-scale mapping of dynamic biomechanical tissue properties," *Opt. Express* **16**(15), 11052–11065 (2008).
107. K. M. Kennedy et al., "Needle optical coherence elastography for tissue boundary detection," *Opt. Lett.* **37**(12), 2310–2312 (2012).
108. M. R. Ford et al., "Method for optical coherence elastography of the cornea," *J. Biomed. Opt.* **16**(1), 016005 (2011).
109. X. Liang and S. A. Boppart, "Biomechanical properties of in vivo human skin from dynamic optical coherence elastography," *IEEE Trans. Biomed. Eng.* **57**(4), 953–959 (2010).
110. B. F. Kennedy et al., "In vivo three-dimensional optical coherence elastography," *Opt. Express* **19**(7), 6623–6634 (2011).
111. R. K. Chhetri et al., "Magnetomotive optical coherence elastography for relating lung structure and function in cystic fibrosis," *Proc. SPIE* **7554**, 755420 (2010).
112. A. S. Khalil et al., "Tissue elasticity estimation with optical coherence elastography: toward mechanical characterization of in vivo soft tissue," *Ann. Biomed. Eng.* **33**(11), 1631–1639 (2005).
113. R. C. Chan et al., "OCT-based arterial elastography: robust estimation exploiting tissue biomechanics," *Opt. Express* **12**(19), 4558–4572 (2004).

114. J. Rogowska et al., "Optical coherence tomographic elastography technique for measuring deformation and strain of atherosclerotic tissues," *Heart* **90**(5), 556–562 (2004).
115. G. van Soest et al., "Robust intravascular optical coherence elastography by line correlations," *Phys. Med. Biol.* **52**(9), 2445–2458 (2007).
116. X. Liang, V. Crecea, and S. A. Boppart, "Dynamic optical coherence elastography: a review," *J. Innov. Opt. Health Sci.* **3**(4), 221–233 (2010).
117. X. Liang et al., "Acoustomotive optical coherence elastography for measuring material mechanical properties," *Opt. Lett.* **34**(19), 2894–2896 (2009).
118. W. Qi et al., "Phase-resolved acoustic radiation force optical coherence elastography," *J. Biomed. Opt.* **17**(11), 110505 (2012).
119. J. Kim, A. Ahmad, and S. A. Boppart, "Dual-coil magnetomotive optical coherence tomography for contrast enhancement in liquids," *Opt. Express* **21**(6), 7139–7147 (2013).
120. V. Crecea et al., "Magnetomotive nanoparticle transducers for optical rheology of viscoelastic materials," *Opt. Express* **17**(25), 23114–23122 (2009).
121. G. van Soest et al., "Robust intravascular optical coherence elastography by line correlations," *Phys. Med. Biol.* **52**(5), 2445–2458 (2007).
122. J. De Boer, T. E. Milner, and J. S. Nelson, "Determination of the depth-resolved stokes parameters of light backscattered from turbid media by use of polarization-sensitive optical coherence tomography," *Opt. Lett* **24**(4), 300–302 (1999).
123. B. H. Park et al., "In vivo burn depth determination by high-speed fiber-based polarization sensitive optical coherence tomography," *J. Biomed. Opt.* **6**(13), 474–479 (2001).
124. S. K. Nadkarni et al., "Measurement of collagen and smooth muscle cell content in atherosclerotic plaques using polarization-sensitive optical coherence tomography," *J. Am. Coll. Cardiol.* **49**(3), 1474–1481 (2007).
125. S. D. Giattina et al., "Assessment of coronary plaque collagen with polarization sensitive optical coherence tomography (PS-OCT)," *Int. J. Cardiol.* **107**(11), 400–409 (2006).
126. W. C. Kuo et al., "Assessment of arterial characteristics in human atherosclerosis by extracting optical properties from polarization-sensitive optical coherence tomography," *Opt. Express* **16**(12), 8117–8125 (2008).
127. W. Y. Oh et al., "Single-detector polarization-sensitive optical frequency domain imaging using high-speed intra a-line polarization modulation," *Opt. Lett.* **33**(2), 1330–1332 (2008).
128. W. Y. Oh et al., "High-speed polarization sensitive optical frequency domain imaging with frequency multiplexing," *Opt. Express* **16**(6), 1096–1103 (2008).
129. M. Villiger et al., "Artifacts in polarization-sensitive optical coherence tomography caused by polarization mode dispersion," *Opt. Lett.* **21**, 4 (2013).
130. M. Villiger et al., "Spectral binning for mitigation of polarization mode dispersion artifacts in catheter-based optical frequency domain imaging," *Opt. Express* **21**(9), 2445–2458 (2013).